A numerical model for the fluid structure interaction of a three-dimensional net structure.

A. Fredheim* and O. M. Faltinsen†

November, 2001

Abstract

A three-dimensional numerical model of the fluid flow, including structural analysis, which takes into consideration the influence of the net structure on the flow, has been developed. The net is divided into a set of cylindrical and spherical elements to represent the twines and knots, respectively, where each of these different elements are modeled as a set of source distributions and single point sources. To determine the strength of these sources we apply the principle of Lagally, which basically states that the force acting on a source of strength q in uniform flow is equal to the source strength times the incoming velocity times the fluid density. Thus we get a set of equations describing the relation between the fluid velocity and the source strength at every element. This means that we get a model which describes the disturbance of the fluid flow due to the presence of the net.

In this paper, results from numerical simulation of net panels will be presented. These results will be validated against model test results. For the fluid flow through three-dimensional net structures however, there are limited published results. Therefore only measurements of drag on nets will be used as verification.

1 Introduction

The resources of wild fish are limited. The trend in recent years has been that the amount of wild catch is stagnating. In this perspective the selectivity of fishing gear has become an important issue. The research so far has mainly focused on the testing of different sorting devices. In addition, numerical models have been developed to study the shape and behavior of both trawls and purse seines. All of these numerical models known to the authors are based on the assumption of undisturbed flow, both in front and inside the net structure. A three-dimensional net structure is however a highly flexible structure and the force acting on the structure due to the fluid flow will have an affect on the shape of the structure, and further will alter the influence of the net structure on the fluid flow.

We are calculating the influence from the net on the fluid flow in this article by representing the wake generated by each element as source distributions along the structural element. If some elements are in the wake of other elements, we do not correct for the reduced inflow due to velocity deficit in the wake. Taking as an example a plane net in a uniform ambient flow with no velocity component parallel to the net, this model is appropriate for an angle of attack between 90 and approximately 25 degrees. If we assume that the plane net is situated in the yz-plane, then by angle of attack is meant the angle between the ambient flow direction, restricted to be in the xy-plane and the plane through the the net. This is illustrated in figure 1.

The idea then is to correct for the wake inflow on each of the cylinders due to the presence of all the other cylinders and to be able to do this without implying a large model based on a structural finite element method or a CFD method based on Reynolds averaged Navier-Stokes equations. The latter will in practise be impossible due to the required CPU time and data storage. A structural analysis of the net

*Department of Aquaculture Technology, SINTEF Fisheries and Aquaculture, Norway

†Department of marine hydrodynamics, Norwegian Institute of Science and Technology, Norway

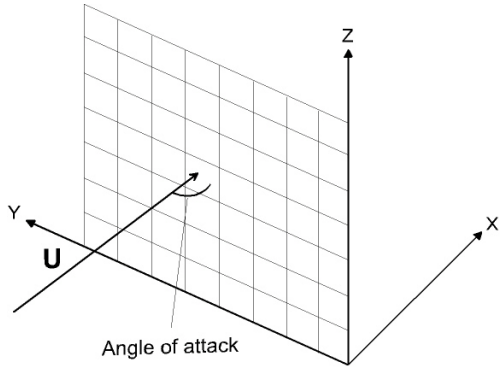

Figure 1: Definition of angle of attack used in this article. It is assumed that the ambient inflow vector is restricted to be in the xy-plane.

structure using bar elements has been included in the model. By combining the change in the inflow due to the presence of the net structure, which is a function of the shape and geometry of the net, with a correction of the shape and geometry due to the drag load, we get a more complete description of the problem.

2 Modeling

2.1 Fundamentals

Figure 2 illustrate two different types of net panels, a square mesh and diamond mesh type. In net pens, used for aquaculture purposes, the square mesh type is mainly used, while in trawling normally the diamond mesh structures is used. The use of diamond mesh structures is favored in trawling, because when the trawl is exposed to forces the mesh opening will become smaller and the forces will be distributed within the twine structure in a more persistent way. But this also implies that there is less control of the actual opening of mesh while trawling, which is important with regards to selectivity. It is important to be aware that geometrical elasticity, which is important for a net structure, is not modeled. The elasticity of the material in the net is though an input parameter, such that it is possible to change this to try to get a best description of the physical properties. But describing the accurate elasticity of the net structure is beyond the scope of this work. Geometrical elasticity is a very important factor while discussing the differences between a square and diamond mesh structure. This can be qualitatively understood by just pulling on each side of a net with different types of mesh. This also make it difficult or impossible to compare results from a numerical analysis with square mesh, with experiments performed on a diamond mesh structure, when considering the geometry.

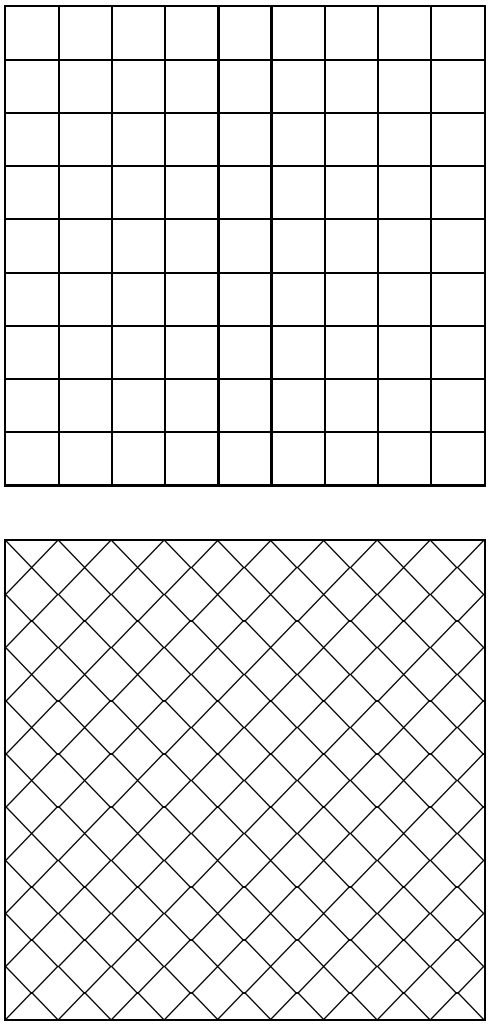

Figure 2: Illustration of square mesh (top) and diamond mesh nets(bottom)

We decided to divide the three-dimensional net structure into discrete elements. First we started out by modeling the twines as separate cylinders between knots, with two-dimensional properties, allowing the interaction between

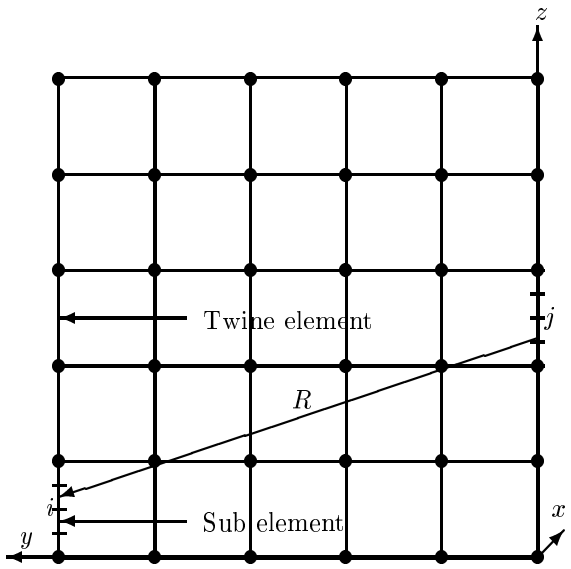

Figure 3: Illustration of modeling of the net

them to be three-dimensional. Later we added the knots into the model, modeling them as separate spheres, with full three-dimensional properties. The reason for this is explained later. The modeling is illustrated in figure 3. In this article, the cylinders and spheres are named twine elements and knot elements respectively. Each of the twine elements between knots can further, but do not have to, be divided into sub elements, as illustrated in the figure. In the following, we do not distinguish between twine elements and sub elements, if not specifically stated that we are discussing sub elements. The total drag on the net will then become a sum of the drag of each of the individual elements. The net is assumed undeformable in the following analysis.

The drag on each of the elements are calculated using standard drag formulation. As is well known, the drag on a single circular cylinder in a two-dimensional free flow can be calculated knowing the drag coefficient for the cylinder by $\mathbf{F_c} = 1/2\rho C_D D L|\mathbf{U}|\mathbf{U}$, where $\mathbf{U}$ is the inflow velocity vector in a plane orthogonal to the cylinder axis. $|\mathbf{U}|$ is the magnitude of the inflow velocity, D is the diameter and L is the length of the cylinder. The expression for the drag on a sphere in three-dimensional free flow will in a similar fashion become $\mathbf{F_s} = \pi D^2/8 C_D \rho |\mathbf{U}_{3D}|\mathbf{U}_{3D}$, where $\pi D^2/4$ is the projected area of the sphere.

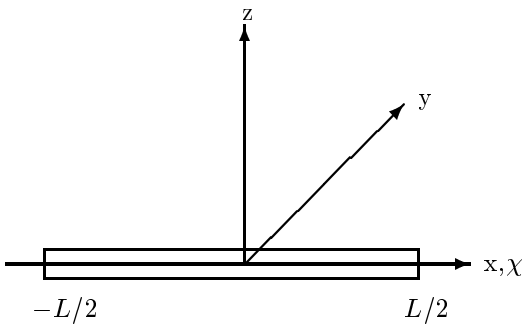

Figure 4: Definition of local axis system for a two dimensional slender body element.

The next sections will describe how we model the disturbance from the individual elements on the flow and the interaction effect between the elements. This part assumes implicitly that no elements are in the wake of other elements.

2.2 Disturbance potential

We assume that the fluid is incompressible. We define a time average wake behind each twine and knot. Outside of this wake, the fluid is assumed inviscid and the fluid motion irrotational. I.e. a velocity potential can be used to describe the fluid velocity, $\mathbf{U} = \nabla\phi$. This velocity potential will then satisfy the Laplace equation $\nabla^2\phi = 0$. The presence of the wake is modeled by sources centered in the twines and knots.

Let us first consider a twine element between two knots. The dominant far-field solution, outside the wake, of the velocity potential at point (x, y, z) due to the disturbance of the twine, can be represented as:

$$\phi_c(x, y, z, \chi) = \frac{1}{4\pi}\int_{-L/2}^{L/2} \frac{q(\chi)}{\sqrt{(x-\chi)^2 + y^2 + z^2}} d\chi \quad (1)$$

Definitions are given in figure 4.

And similarly the disturbance from the knot elements can be modeled as a three-dimensional

point source:

$$\phi_s(x,y,z) = \frac{1}{4\pi}\frac{Q}{\sqrt{x^2+y^2+z^2}} \tag{2}$$

The unknown in these equations are the source strength distribution for the twine elements and the source strength for the knot elements. To find an relation between the source strength and the drag force on the element, we use the Lagally's theorem.

2.3 Lagally's theorem

Basically Lagally's theorem state that the force acting on a source of strength q in uniform flow can be expressed as:

$$\mathbf{F} = \rho q \mathbf{U} \tag{3}$$

The theorem is valid both in two and three dimensions. More about Lagally's theorem in [9]. If we then assume that the flow around a cylinder in free flow with diameter D can be represented by an equivalent source of strength q and then apply the ordinary viscous force formulation for a cylinder in free flow ([12] and [1]), we get:

$$\mathbf{F} = \frac{1}{2}\rho C_d D|\mathbf{U}|\mathbf{U} = \rho q \mathbf{U} \tag{4}$$

We then have established a relation between the source strength and the incoming flow $\mathbf{U}$, when the source is a representation of the cylinder:

$$q = \frac{1}{2}C_D D|\mathbf{U}| \tag{5}$$

2.4 Equation system

With equations (1), (2) and (5) we now have the necessary relations to establish a system of equations to solve the problem. We apply equation (5) at the center of every element (twines, including any possible sub elements and knots) in the net structure, where $\mathbf{U}$ will be a function of the incoming free flow $\overline{\mathbf{U}}$ and the sum of the disturbance $\mathbf{u}$, from all the other elements. The disturbance from each individual element is given by equation (1) and (2). We then get a set of equations where the unknown source strength q for a twine element i is given as a function of the influence of all the other elements (see figure 3). We will similarly get a set of equations for the unknown source strength Q for every knot element.

The equations for element i will then become as follows for the twine elements and knot elements respectively:

$$q_i = \frac{(C_D D L)_i}{2}\left|\overline{\mathbf{U}}_i + \sum_{j=1\neq i}^{N_c}\mathbf{u}_{cj} + \sum_{k=1}^{N_s}\mathbf{u}_{sk}\right|_{2D} \tag{6}$$

$$Q_i = \frac{(C_D D^2)_i}{8}\left|\overline{\mathbf{U}}_i + \sum_{j=1}^{N_c}\mathbf{u}_{cj} + \sum_{k=1\neq i}^{N_s}\mathbf{u}_{sk}\right|_{3D} \tag{7}$$

where D is the diameter of the twine or knot element, L is the length of the twine element, $\mathbf{u_{cj}}$ is the disturbance from the twine elements j, $\mathbf{u_{sk}}$ is the disturbance from the knot element k, N_c is the number of twine elements and N_s is the number of knot elements. We then have a total of $N_c + N_s = N$ elements. There is no influence from the i element on itself, thus the element index i is removed from the sum in the equations. For the twine element it is the decomposed 2D velocity in the plane perpendicular to the element i which is used in the equation. I.e. $\overline{\mathbf{U}} = <\overline{U}_x, \overline{U}_y>$ and $\mathbf{u} = <u_x, u_y>$

Since the right hand side of the equations involve the scalar of the velocity vector we get the following square system to solve for the unknown source strength:

$$\begin{aligned} q_i^2 \quad = \quad & \left(\frac{(C_D D L)_i}{2}\left(\overline{U}_{xi} + \sum_{j=1\neq i}^{N_c} u_{cxj}\right) + \right. \\ & \left.\frac{(C_D D^2)_i}{8}\sum_{k=1}^{N_s} u_{sxk}\right)^2 + \\ & \left(\frac{(C_D D L)_i}{2}\left(\overline{U}_{yi} + \sum_{j=1\neq i}^{N_c} u_{cyj}\right) + \right. \\ & \left.\frac{(C_D D^2)_i}{8}\sum_{k=1}^{N_s} u_{syk}\right)^2 \end{aligned} \tag{8}$$

For the sake of simplicity the sum of the influences from the twine and knot elements ($\sum u_{c/s}$) are denoted u and the constants are removed in the following equation. Equation (8) can then be written as:

$$q_i^2 = \Big(\overline{U}_x^2 + \overline{U}_y^2 + 2\overline{U}_x u_x + 2\overline{U}_y u_y + u_x^2 + u_y^2\Big) \quad (9)$$

We see that the equation consist of one part due to the undisturbed uniform flow, one part solely due to the disturbance and one term including both the uniform velocity and the disturbance. If we assume that uniform flow is of $O(1)$ and that the disturbance is of $O(\epsilon)$, the three parts will be of $O(1)$, $O(\epsilon^2)$ and $O(\epsilon)$, respectively. It would then be tempting to remove all terms of $O(\epsilon^2)$. But this would result in a model where we would get no interaction between the elements for a flat net in the yz-plane with a uniform flow in the x-direction. Thus we keep terms of $O(\epsilon^2)$.

2.5 Velocities

We are solving for the unknown source strengths q_i and Q_i, by introducing the disturbance from the other elements as the velocity in equation (8). The velocities are then given by differentiating the disturbance potentials given in subsection 2.2. In a local coordinate system for the twine element j as given in figure 4, we get for the x,y, and z-velocities (index c indicates twine element):

$$\frac{\partial \phi}{\partial x} = u(x,y,z;\chi)_{cx} = \frac{1}{4\pi}\int_{-L/2}^{L/2} \frac{q(\chi)(x-\chi)}{(x^2 - 2x\chi + \chi^2 + y^2 + z^2)^{3/2}} d\chi \quad (10)$$

$$u(x,y,z;\chi)_{cy} = \frac{1}{4\pi}\int_{-L/2}^{L/2} \frac{q(\chi)y}{(x^2 - 2x\chi + \chi^2 + y^2 + z^2)^{3/2}} d\chi \quad (11)$$

$$u(x,y,z;\chi)_{cz} = \frac{1}{4\pi}\int_{-L/2}^{L/2} \frac{q(\chi)z}{(x^2 - 2x\chi + \chi^2 + y^2 + z^2)^{3/2}} d\chi \quad (12)$$

and the disturbance from the knot elements which are given in global coordinate system becomes (index s indicates twine elements):

$$u(x,y,z)_{sx} = \frac{1}{4\pi}\frac{Qx}{(x^2+y^2+z^2)^{3/2}} \quad (13)$$

$$u(x,y,z)_{sy} = \frac{1}{4\pi}\frac{Qy}{(x^2+y^2+z^2)^{3/2}} \quad (14)$$

$$u(x,y,z)_{sz} = \frac{1}{4\pi}\frac{Qz}{(x^2+y^2+z^2)^{3/2}} \quad (15)$$

In general the integrals has to be solved numerically for a given distribution of $q(\chi)$ along the element. But if we assume that the source strength is constant over the element, we can analytically solve equations (10), (11) and (12) for the velocities in x,y and z direction when the element is situated along the x-axis:

$$u(x,y,z)_{cx} = \frac{q}{4\pi}\frac{(\%1 - \%2)}{\%3\%4} \quad (16)$$

$$\%1 = \sqrt{x^2 + xL + L^2/4 + y^2 + z^2}$$
$$\%2 = \sqrt{x^2 - xL + L^2/4 + y^2 + z^2}$$
$$\%3 = \sqrt{x^2 - 2xL + L^2/4 + y^2 + z^2}$$
$$\%4 = \sqrt{x^2 + 2xL + L^2/4 + y^2 + z^2}$$

$$u(x,y,z)_{cy} = \frac{-qy}{4\pi}\frac{1}{\%2\%5} + \frac{qy}{4\pi}\frac{1}{\%1\%6} \quad (17)$$

$$\%5 = (L/2 - x + \sqrt{x^2 - xL + L^2/4 + y^2 + z^2})$$
$$\%6 = (-L/2 - x + \sqrt{x^2 + xL + L^2/4 + y^2 + z^2})$$

2.6 Numerical solution procedure

We have a non-linear equation system to solve for the unknown source strength and to do this we have to apply an iterative solution scheme. A very common scheme to use is the Newton-Raphson iterative method. This method involves solving an ordinary $\mathbf{Ax} = \mathbf{B}$ equation system for each iteration step.

We have for each of the elements an equation of the following type:

$$F_i(q_1 \dots q_{Nc}; Q_1 \dots Q_{Ns}) = F_i(\mathbf{q}) = 0 \quad (18)$$

With a Taylor expansion around $\mathbf{q}$ we get:

$$F_i(\mathbf{q} + \delta\mathbf{q}) = F_i(\mathbf{q}) + \sum_{j=1}^{N} \frac{\partial F_i(\mathbf{q})}{\partial q_j} \delta q_j + O(\delta\mathbf{q}^2) = 0 \quad (19)$$

And for all the $N_c + N_s$ equations together:

$$\mathbf{F}(\mathbf{q} + \delta\mathbf{q}) = \mathbf{F}(\mathbf{q}) + \mathbf{J}\delta\mathbf{q} + O(\delta\mathbf{q}^2) = 0 \quad (20)$$

where $\mathbf{J}$ is the Jacobian of the equation system. The solution to be solved for every iteration step is then:

$$\mathbf{J}\delta\mathbf{q} = -\mathbf{F}(\mathbf{q}) \quad (21)$$

where the solution of the equation is $\delta\mathbf{q}$. For every step the source strength on the right hand side is $\mathbf{q}_{new} = \mathbf{q}_{old} + \delta\mathbf{q}$.

2.7 Convergence

In principle, if we increase the number of sub elements which each of the twine elements are divided into (refer to subsection 2.1 and figure 3), the result should converge towards an asymptotic value, as the equation system is more accurately described. In our case, when modeling only the twines and not the knots, we actually experienced a divergence in the result as the number of sub elements increased. This is shown in figure 5. Here we see the total drag on a simple square net with 2x2 twines increase as the number of elements along the twines are increased. The explanation is that, while increasing the number of sub elements, such that the size of each sub element is decreased, at the corners (the knots) where the twines intersect, the center of the elements of the different twines and thereby the singularities become very close. This in addition lead to large influences between the elements and the result diverge.

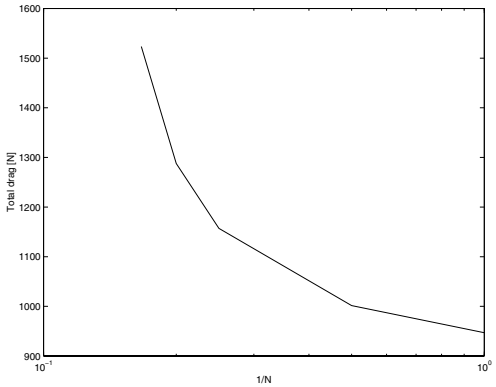

Figure 5: Total drag (-) on a square net with 2x2 twines and without knots, as a function of no. of elements. Uniform flow perpendicular to the net plane.

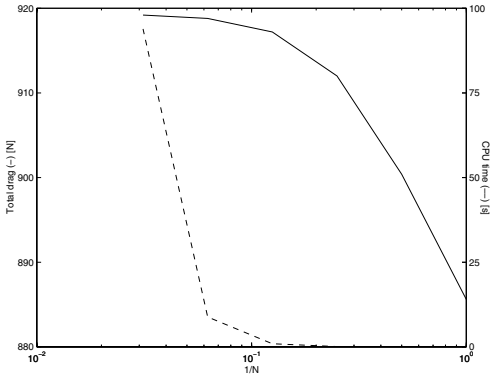

Figure 6: Total drag (-) and CPU time (- -) on a square net with 2x2 twines and with knots, as a function of no. of elements. Uniform flow perpendicular to the net plane.

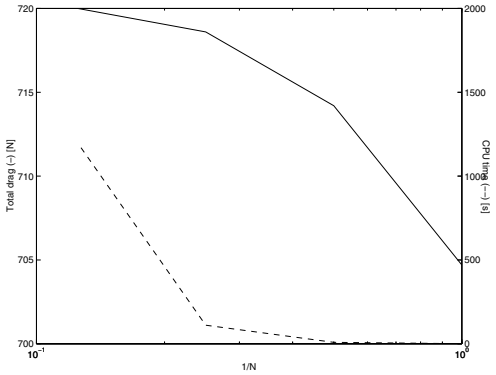

Figure 7: Total drag (-) and CPU time (- -) on a square net with 5x5 twines and with knots, as a function of no. of elements. Uniform flow perpendicular to the net plane.

While adding the knot elements to the description, allowing for modeling the knots, this problem is solved. The twine elements and thereby the singularities in the corners, will then be separated by the physical size of the knot element. In figure 6 results with the knots included are presented. As seen the results for the total drag on the net are converging as the number of elements are increased. In figure 7 similar results are presented for a net with a 5x5 twines. For these calculations a drag coefficient of 1.2, a diameter of 0.3 [m] for both the twines and the knots and an uniform velocity of 1.0 [m/s] is used.

Further we see that the CPU time increase with increasing number of elements. Due to the iterative solution procedure described in section 2.6 the CPU time is proportional with N^3.

2.8 Further modeling

Due to the N^3 proportionality with CPU time some work has been done on alternative descriptions of the source strength distribution, to increase the efficiency of the model. Motivated by the shape of the discrete source distribution presented in figure 8 for the twine elements and figure 9 for the knot elements, two different approaches have been tried out. These approaches are to represent the source distribution over the net as a Fourier series and as a B-splines distribution. The idea is to be able to represent the source distribution across the complete twine (not separated into twine elements between the knots) and even the complete net structure, described by a set of parameters.

Modeling by means of Fourier series Results show that the source strengths between the elements have a distribution which seems suitable for a Fourier series representation. I.e. instead of assuming a constant source strength over each individual twine element, we assume a source distribution along each complete twine.

$$q(\chi) = a_0 + \sum_{n=1}^{\infty} (a_n \cos(nx) + b_n \sin(nx)) \tag{22}$$

This can be found in standard mathematical textbooks like for instance [4]. So instead of solving for the unknown $q(\chi)$, we solve for the unknown coefficients a_n and b_n. The idea is to represent a larger number of twine elements by a single series. The downside is that it is no longer possible to solve the integral for the velocities analytically, but it has to be solved by numerical integration. In figure 10 a comparison between the discrete distribution using 20 elements and the source strength represented by a 6 component Fourier series is shown. The physical size of the net is 20 by 20 [m], which is modeled using 21 by 21 twines, with a diameter of 0.05 [m]. The drag coefficient is 1.0 and a the magnitude of the uniform flow is 10 [m/s]. As seen there is a good agreement between the two solutions.

It is also possible to use one single two dimensional Fourier series to describe the source distribution over the net plane:

$$q(\chi, \eta) = a_0 + \sum_{m=1}^{\infty} \sum_{n=1}^{\infty} (a_{mn} \cos(mx) \cos(ny) + b_{mn} \sin(mx) \sin(ny)) \tag{23}$$

Even though it is possible to get a good representation of the source distribution using the Fourier series representation with significantly fewer unknowns, (as shown in figure 10), due to the numerical solution of the integrals needed to solve equation (10), (11) and (12), the overall task become more time consuming. Thus the discrete formulation are preferred.

B-spline representation Another similar and possible approach would be to represent the source distribution by using B-splines. Equation (24) show the basic formulation of a B-spline. A good textbook describing the principle behind

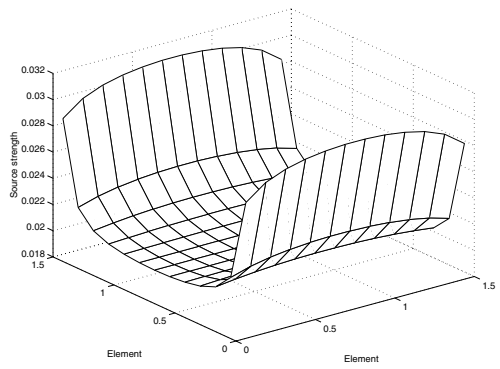

Figure 8: Source strength distribution for the twine elements along the complete twines parallel to y-axis. A net made up of of 13 by 13 twines is used.

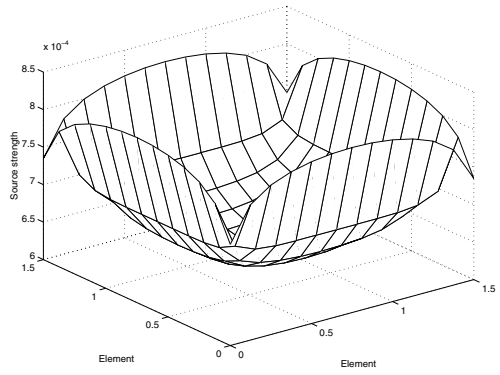

Figure 9: Source strength distribution for the knot elements. A net made up of of 13 by 13 twines is used.

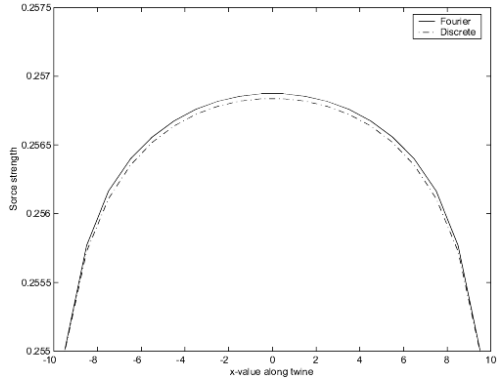

Figure 10: Comparison between Fourier and discrete solution of the source strength. The solution is based on 20 discrete elements and 6 fourier components.

B-splines is [10]. This approach has been used in other marine hydrodynamic application with success (for instance [7]), to be able to solve complicated problems in a robust and efficient manner.

$$P(t) = \sum_{i=1}^{n+1} B_i N_{i,k}(t)$$
$$t_{min} <= t < t_{max},\ 2 <= k <= n+1 \quad (24)$$

2.9 Structural formulation

We assume that the net structure can be modeled as a set of node points with completely stiff elements in between. We are then able to use the same element model for the twines as described in subsection 2.1, including the possibility of adding sub elements, which will allow for flexibility between the knots or nodes. The length of the elements will remain constant, and this fact is used to be able to solve the system. The unknown will then be the equilibrium force in each element and the coordinates of each node. For each element we then have six unknown coordinates and one unknown tension and six equation of equilibrium (three in each node) and one equation stating the distance between the two nodes has to remain constant. I.e. elasticity in the material and stretching is not accounted for. We then have a static definite system.

All loads on each element are distributed with half in each node. External loads include weight, drag and any given load. Looking at node k with n connecting elements i, we denote the drag force from each element D_i, the tension in each element T_i, the weight per meter w_i, length of element l_i and external loads at the node as R. We then get the following relations for the equilibrium of each node:

$$f_{x,k} = \sum F_{x,k} = 0 \Rightarrow \quad (25)$$
$$\sum_{i=1}^{n} \frac{T_i}{l_i} (\mathbf{x}_i - \mathbf{x}_k) + \sum_{i=1}^{n} \frac{D_{x,i}}{2} + R_x = 0$$

$$f_{y,k} = \sum F_{y,k} = 0 \Rightarrow \sum_{i=1}^{n} \frac{T_i}{l_i} (\mathbf{y}_i - \mathbf{y}_k) + \sum_{i=1}^{n} \frac{D_{y,i}}{2} + R_y = 0 \quad (26)$$

$$f_{z,k} = \sum F_{z,k} = 0 \Rightarrow \sum_{i=1}^{n} \frac{T_i}{l_i} (\mathbf{z}_i - \mathbf{z}_k) + \sum_{i=1}^{n} \frac{D_{z,i}}{2} + R_z = 0 \quad (27)$$

$$g_i = (x_2 - x_1)_i^2 + (y_2 - y_1)_i^2 + (z_2 - z_1)_i^2 - l_i^2 = 0 \quad (28)$$

More about this in [5] for general applications and with applications to trawls in [13].

Since equation 28 is non-linear it is not straight forward to solve the system. We have to use a numerical solution procedure. The most common is the Newton-Raphson iterative scheme as described in 2.6. By doing a Taylor expansion of the four equations with respect to the unknown tension an node coordinates we get a set of linear equation which we can solve for each iteration step:

$$\frac{\partial}{\partial T_i}(f_{x,k}) = \frac{(x_i - x_k)}{l_i}$$
$$\frac{\partial}{\partial T_i}(f_{y,k}) = \frac{(y_i - y_k)}{l_i}$$
$$\frac{\partial}{\partial T_i}(f_{z,k}) = \frac{(z_i - z_k)}{l_i} \quad (29)$$

$$\frac{\partial}{\partial x_i}(f_{x,k}) = \frac{T_i}{l_i} \; ; \; \frac{\partial}{\partial y_i}(f_{y,k}) = \frac{T_i}{l_i}$$
$$\frac{\partial}{\partial z_i}(f_{z,k}) = \frac{T_i}{l_i}$$
$$\frac{\partial}{\partial x_k}(f_{x,k}) = -\frac{T_i}{l_i} \; ; \; \frac{\partial}{\partial y_k}(f_{y,k}) = -\frac{T_i}{l_i}$$
$$\frac{\partial}{\partial z_k}(f_{z,k}) = \frac{T_i}{l_i} \quad (30)$$

with

$$\frac{\partial}{\partial x_i}(g_i) = 2(x_i - x_j) \; ; \; \frac{\partial}{\partial y_i}(g_i) = 2(y_i - y_j)$$
$$\frac{\partial}{\partial z_i}(g_i) = 2(z_i - z_j)$$
$$\frac{\partial}{\partial x_k}(g_i) = -2(x_i - x_j) \; ; \; \frac{\partial}{\partial y_k}(g_i) = -2(y_i - y_j)$$
$$\frac{\partial}{\partial z_k}(g_i) = -2(z_i - z_j) \quad (31)$$

We then get for every iteration step a $\mathbf{Ax} = \mathbf{B}$ equation system. Boundary conditions are imposed by removing the row and column corresponding to the known coordinates.

Also an alternative FEM formulation is included, based on modeling the twines as structural bar elements. This model will not be described here, but a good reference would be [5].

2.10 Comments on the modeling

First is described a method, which accounts for the presence of the net by calculating the interaction between the different elements of a net structure, correcting for the inflow on each element. No elements are assumed to be in the wake of other elements. Secondly a structural description and analysis of the net is included, allowing for calculating a new geometry of the net due to the incoming flow. Based on this new geometry, a new correction of the inflow can be calculated and it is possible to continue on until some kind of requirement is met. Bearing in mind that both the part involving calculating the new inflow and the calculation of the new geometry involves solving non-linear equations, this ends up being a time consuming task.

3 Verification

3.1 Results as a function of the solidity ratio

In figure 11 are presented the drag on a plane net situated at a 90 degree angle to the free flow as a function of the solidity ratio, Sn of the net. Sn is defined as the ratio between the projected area A_n of the net and the total area A enclosed by the net. Four different results are presented as non-dimensional drag, which is obtained by dividing the results with $1/2\rho A|\overline{\mathbf{U}}|^2$. The results by Løland [6] are based on an empirical formulation, which again is based on experiments by towing plane nets with different solidity ratios through a towing tank at different velocities. The results by Milne are based on the formulation presented in his paper [8]. The results named "Uniform", are a sum of the viscous drag of all the elements with no correction of the inflow. The results named "Inflow correction" are similarly a sum of the viscous drag of all the elements, but with the inflow velocity corrected based on the formulation in this paper. For the calculations are used a drag coefficient of 1.15, a diameter of the twines of 0.02 [m] and the magnitude of the uniform flow is 1.0 [m/s]. Thus for the calculations the Reynolds number, Rn, is 20000 at 20 degree C.

As seen there is some discrepancy in the results compared to the results of Løland, especially for higher solidity ratios. The discrepancy between our results and the results by Milne is on the other hand not that large. Some comments related to these results:

- The empirical formulation by Løland is based on experiments with a solidity range from 0.130 to 0.317, and is "optimized" for the middle solidity range. Thus at the higher solidity range the results might not be a good comparison. The results of Milne is based on an analytical formulation and is also verified against nets with a relatively low range of solidity ratio.
- Secondly due to the nature of a net structure, it will not be possible during experiments to avoid some deformation, which again will have an influence on inflow of the net and thereby the resulting drag force. Deformation of the net is not accounted for in the "inflow correction" results presented in this paper.
- At high solidity ratios the interaction effects will become more important, since it will be relatively more material present that obstruct the flow of water. This should favor a model that consider the change in the inflow velocity due to the presence of the net structure itself.
- The formulation of Løland is a third order equation with respect to solidity ratio, while the formulation which Milne based his findings on is a second order equation with respect to the solidity ratio. I.e. when increasing the solidity ratio out of the "optimum" range for the actual model, the effect on the results is large, which might limit its validity in this region.

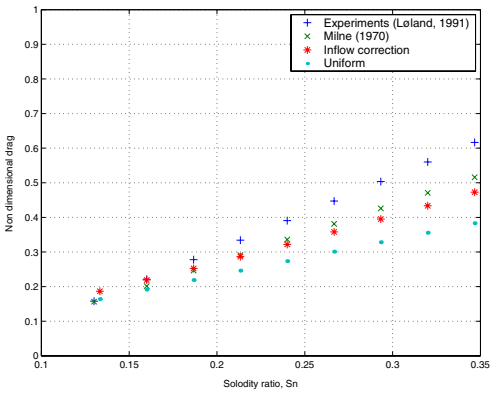

Figure 11: Non-dimensional drag on a plane net structure as a function of the solidity ratio, Sn

3.2 Results as a function of angle of attack

In figure 12 results for the drag on a plane net at different angles of attack is presented. The definition of angle of attack is given in section 1 and figure 1. Three different results are presented. The results by Løland [6] are based on the same assumptions as described earlier, with the dependency of angle of attack also derived from experiments. The results presented here are based on a net with a solidity ratio of 0.2667,

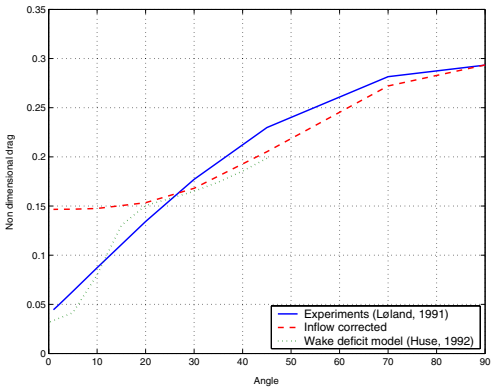

Figure 12: Non-dimensional drag on a plane net as a function angle of attack. The solidity ratio is 0.2667

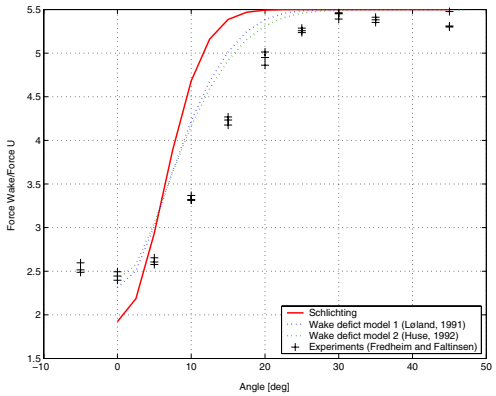

Figure 13: The non-dimensional drag force on five cylinders in a row, calculated using different wakefield models, compared to experiments as a function of angle of attack.

a drag coefficient of 1.0 and the magnitude of the uniform velocity of 1.0. This curve is fitted to the result of the "inflow correction" method at the 90 degree angle of attack. The argument for this is to give a representation of the results which is easier for comparison between the models in view of the change in drag force and not the absolute drag force as a function of attack.

As seen the asymptotic value for the "inflow correction" model, when the angle of attack approaches zero, is approaching a non zero value which is much larger than the results by Løland. The asymptotic value is approximately equivalent to the sum of the drag on each of the vertical cylinders modeling the vertical twines of the net with no correction of the inflow velocity on the elements. The drag on the horizontal twines of the net will be equal to zero in the present model, since the decomposed velocity vector in the local coordinate system of the horizontal twine elements will be equal to zero. The third results, named "Wake deficit model", is a model that accounts for the reduced inflow due to the velocity deficit in the wake behind a cylinder in flow and the added effect of several cylinders situated in a row behind each other with respect to the inflow direction. Some remarks regarding the results:

- We see that down to an angle of attack of approximately 25 degrees the two models follow each other relatively good, at least the trend is similar. But at lower angles the two curves divide, due to reasons explained earlier. This illustrate the need of including a wake field model that is able to calculate the influence between the different parts of the net at low angles of attack.

- One such possible formulation, "Wake deficit model" [3], is included in the figure as a reference. This model is based on the formulation by Schlichting [11] and is modified to account for the added effect of several cylinders in the flow field and their individual position in the generated wake field.

- As described previously due to the nature of a net structure, it will not be possible during experiments to avoid some deformation of the net itself, which again will not only have an influence on inflow of the net and thereby the resulting drag force, but also on the "effective" angle of attack. Deformation of the net is not accounted for in the "inflow correction" results presented in this paper.

- There are several uncertainties connected to the results presented in this figure. Looking at the experiments for which the model of Løland is based on, it is not carried out any experiments between the angle of 10 and 30 degrees. And as seen from the "Wake deficit model" results, there are indications that in this region, large changes in the velocity field with respect to angle of attack are occurring.

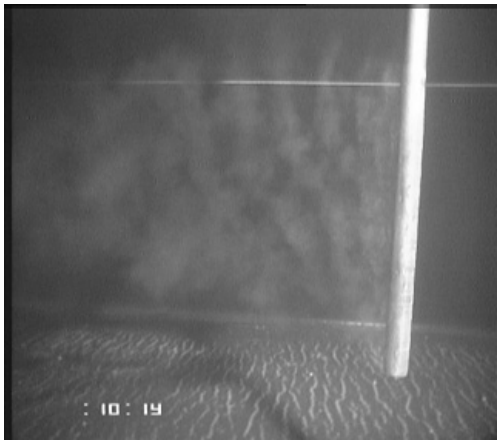

Figure 14: Visualization of three dimensional flow behind a single cylinder, while towed at constant speed through a towing tank.

To get a better understanding of the different effects in this region, experiments have been carried out. It is not considered a part of this paper to get into details regarding this topic, but some findings will briefly be described. The results are presented in figure 13 together with three different wake deficit models. The diameter, D of the cylinders are 0.04 [m], the height, h, is 0.8 [m] and for the wake deficit models a drag coefficient of 1.1 is used. The results are made non-dimensional by dividing with $1/2\rho Dh|\overline{\mathbf{U}}|^2$. One of the problems constructing such a wake model is how to sum up the added effect from each individual cylinder on the total wake field. The basis for all the models are the velocity deficit model described by Schlichting [11] with different modifications to better describe the near field behavior. Due to the nature of the experiments carried out, there are also uncertainties related to three-dimensional effects regarding the flow around a cylinders. This is tried to be illustrated in figure 14, where we see an upward circulation at the end of the cylinder, which give a z-variation of the wakefield velocity behind the cylinder. The intention is to present the findings from the experiments and the different wake models in a later paper.

4 Conclusions and further work

We have presented one possible method for calculating the change in inflow velocity, both in magnitude and vector, due to the presence of a net structure. The model has been verified against experiments and other analytical models, as means of calculating the drag on plane nets as a function of solidity ratio and angle of attack. With regard to solidity ratio, the results show reasonable good agreement with the experiments. As for the angle of attack, as shown, down to an angle of approximately 25 degrees, the agreement or trend is not to poor, but below that angle, the two results divide. It is shown that it is a need of a model considering the wakefield behind the twines to be able to calculations this. The idea behind such a model is presented, but describing the details are considered to be beyond the scope of this paper, but will hopefully be presented in a later paper. Further work will also include verification against experiments on cone net structures presented by Enerhaug and Gjøsund [2].

References

[1] J. W. Elder. Steady flow through non-uniform gauzes of arbitrary shape. *Journal of Fluid Mechanics*, 5:355–369, April 1959.

[2] B. Enerhuag and S. H. Gjø sund. Experimental, numerical and analytical studies of flow through reticulate and solid cones. In *Methods for the Development and Evaluation of Maritime Technologies*. University of Rostock, Germany, November 2001.

[3] Erling Huse. Current forces on individual elements of riser arrays. In *Proceedings of the Second International Offshore and Polar engineering Conference*, June 1992.

[4] Erwin Kreyszig. *Advanced Engineering Mathematics*. John Wiley & Sons, Inc., 7th edition, 1993.

[5] John W. Leonard. *Tension structures : behavior and analysis*. McGraw-Hill, New York, 1988.

[6] G. Løland. *Current forces on and flow through fish farms.* PhD thesis, The Norwegian Institute of Technology, 1991.

[7] H. Maniar. *A three dimensional higher order panel method based on B-splines.* PhD thesis, The Massachusetts Institute of Technology, 1995.

[8] P. H. Milne. Fish farming: A guide to the design and construction of net enclousures. *Department fo Agriculture and fisheries for Scotland, Marine Research*, 1, 1970.

[9] L. M. Milne-Thomson. *Theoretical Hydrodynamics.* Macmillian & Co. Ltd., 1968.

[10] David F. Rogers and J. Alan Adams. *Mathematical Elements for Computer Graphics.* McGraw-Hill, 2nd edition, 1990.

[11] H. Schlichting. *Boundary-Layer Theory.* McGraw-Hill Series in Mechanical Engineering. McGraw-Hill, 1968.

[12] G. I. Taylor. Air resistance of a flat plate of very porous material. *Aeronautical Research Council Reports and Memoranda*, (2236), 1944.

[13] F. Theret. A mathematical model for the determination of the shape and tension of a trawl placed in a uniform current. In *Fish Capture Committee.* International Council for the Exploration of the Sea, 1994.